Increasing CO_2 Storage in Oil Recovery

Kristian Jessen (krisj@pangea.stanford.edu, 650-723-6348)
Linda C. Sam-Olibale (chizoba@pangea.stanford.edu, 650-725-0831)
Anthony R. Kovscek (kovscek@pangea.stanford.edu, 650-723-1218)
Franklin M. Orr, Jr. (fmorr@pangea.stanford.edu, 650-723-2750)
Department of Petroleum Engineering, Stanford University
65 Green Earth Sciences Building
367 Panama Street
Stanford, CA 94305-2220

Introduction

Carbon dioxide (CO_2) injection has been used as a commercial process for enhanced oil recovery (EOR) since the 1970's. Because the cost of oil recovered is closely linked to the purchase cost of the CO_2 injected, considerable reservoir engineering design effort has gone into reducing the total amount of CO_2 required to recover each barrel of oil. If, on the other hand, the objective of the CO_2 injection is to increase the amount of CO_2 left behind at the end of the recovery process, the approach to the design questions changes. In this paper, we consider how CO_2 utilization might be increased.

In the sections that follow we consider several aspects of the design of a CO_2 injection process and ask how each could be modified to increase the use of CO_2. We consider first the composition of the injection gas and the associated concepts of multicontact miscibility that control local displacement efficiency in a gas injection process. We then turn to issues of reservoir flow patterns and consider how operation of the injection processes could be modified. While the design of a particular injection scheme will be quite reservoir specific, the examples given illustrate options that are available to reservoir engineers seeking to increase storage of CO_2.

CO_2 for EOR

Currently, 20,000 tons per day of CO_2 are delivered to oil fields for EOR projects (Moritis 1998). A significant fraction of the injected CO_2 remains in the reservoir, but some is produced along with the oil. Generally, this CO_2 is separated from the oil, recompressed, and injected back into the reservoir. Total production is a little less than 200,000 bbl/d (3.2 $x10^4$ m^3/d) and thus roughly 10 bbl of oil are produced for every ton of CO_2 injected. Most of the CO_2 for EOR originates from naturally occurring geologic traps, although a small fraction is from anthropogenic sources (Stevens and Gale 2000).

To date, CO_2 injection projects have focused on oil with densities between 29 and 48 °API (855 to 711 kg/m^3, respectively) and reservoir depths from 760 to 3700 m (2500 ft to 12000 ft) (Taber *et al.* 1997a). Within the U.S., CO_2-EOR operations are centered in the Permian and Rocky Mountain basins (Texas, New Mexico, and Colorado). Current use of CO_2 for oil recovery is limited by cost and availability of CO_2. If substantial additional quantities of CO_2 are made available due to sequestration efforts, significant CO_2 storage capacity remains to be exploited in oil reservoirs.

Screening criteria have been proposed elsewhere for selecting reservoirs where CO_2 may sustain or increase the production of oil (Taber *et al*. 1997a, Taber *et al*. 1997b). They estimate that upwards of 80% of oil reservoirs worldwide might be suitable for CO_2 injection based upon oil-recovery criteria alone. Moreover, the process is widely applicable in both sandstone and carbonate formations with a variety of permeabilities and thickness of hydrocarbon bearing zones. The major factors limiting CO_2 injection as an oil recovery process have been availability of CO_2 and the cost to build pipelines to carry CO_2 into oil producing regions.

Interactions of Phase Behavior and Flow

The efficiency with which an injected gas (CO_2 or a gas mixture containing CO_2) displaces a liquid such as water or oil depends strongly on the phase behavior of mixtures of the gas with the liquid. As gas is injected into reservoir rock containing oil and water, components present in the gas dissolve in the oil (and to a much lesser extent in the water), while some components present in the oil transfer to the vapor phase. Because the phases present have different saturations, they move at different rates under the imposed pressure gradient, and generally, the lower viscosity vapor phase moves ahead and contacts fresh oil in the reservoir. Those phases mix, equilibrium is established again, and new liquid and vapor phases flow ahead, contacting the fluids in the reservoir. This interaction of phase equilibrium and flow causes components to separate as they propagate through the reservoir in a way that is related to the separations that happen during chromatography.

These chromatographic separations cause the fluid mixtures that form during the displacement to follow a *path* through a composition space of dimension $n_c - 1$, where n_c is the number of components present. When the reservoir pressure is low, gas displaces oil relatively inefficiently (and it displaces water relatively inefficiently at any pressure). If the injection gas composition or the displacement pressure is adjusted appropriately, however, the composition path for gas/oil mixtures can be forced to pass close to the locus of mixture compositions at which the hydrocarbon liquid and vapor phases are critically identical. In such cases, oil can be displaced quite efficiently in the zones invaded by injected gas. These high efficiency displacements are referred to as *multicontact miscible*, a term that is meant to reflect the interplay of phase equilibrium and flow (see Orr *et al*. 1995 for a review of the mathematical theory that describes the development of miscibility). The pressure at which the composition path just reaches the critical locus is called the *minimum miscibility pressure* (MMP). If the injection gas composition is adjusted instead of the pressure, the appropriate quantity is the minimum enrichment for miscibility (MME). Thus, one strategy for increasing CO_2 storage is to displace as much of the oil and water as possible, replacing it with injected gas in the zone swept by the injected gas, and in addition, to make the injected gas as rich as possible in CO_2.

To illustrate how gas composition can be adjusted to increase CO_2 storage, we consider displacement of a specific crude oil by gas mixtures containing varying amounts of CO_2. Table 1 shows the composition of the oil and the basis solvent considered for injection in the study of Zick (1986). The characterization of the components in the injection gas and crude oil used in phase equilibrium calculations with the Redlich-Kwong equation of state is reported by Jessen *et al*. (1998). The injection gas mixtures considered by Zick were created by diluting the solvent containing CO_2, CH_4, ethane (C_2), propane (C_3), butane (C_4), and a small amount of pentane (C_5) with CH_4. The objective of the dilution process was to create an injection gas mixture that would be multicontact miscible at the reservoir temperature (185°F) and the reservoir pressure (3400 psia). The dilution process conserves valuable solvent and increases the volume of injection gas available.

CH_4 was chosen as the dilution gas for the system Zick considered because it was available at the reservoir in question. If CO_2 had been available, however, as it would be if CO_2 sequestration were undertaken on a large scale, then the injection gas could have been made much richer in CO_2. To evaluate the maximum concentration of CO_2 in the injection gas that would still maintain miscible displacement at the reservoir pressure, we calculated the MMP for a series of mixtures of the original solvent with pure CO_2 in place of CH_4. Fig. 1 shows the results. The MMP was calculated by the tie-line intersection technique of Wang and Orr (2001) using the efficient computational approach developed by Jessen *et al.* (1998). That method is based on solutions obtained by the method of characteristics for the conservation equations that describe one-dimensional flow of two-phase, multicomponent mixtures in the absence of dispersion.

Fig. 1 compares MMPs calculated for mixtures of CH_4 and CO_2 with the original solvent mixture. Fig. 1 shows that displacement by the solvent alone would be miscible at a pressure as low as 2100 psia, so dilution of the solvent with some less valuable gas is appropriate. Fig.1 shows also that the solvent can be diluted to a greater extent with CO_2 than it can be with CH_4 and still maintain a MMP of 3400 psia. While displacement with pure CO_2 at 3400 psia and 185°F is not multicontact miscible, less solvent is required to make it miscible than is required if CH_4 is the diluent. Thus, if CO_2 were available, injection gases rich in CO_2 would allow creation of a larger volume of injection fluid for a given availability of solvent.

The impact of replacing the CH_4 in the injection gas with CO_2 on the amount of CO_2 stored per unit volume of pore space filled by injected gas is shown in Fig. 2. Replacing even part of the CH_4 with CO_2 has a significant effect on the storage of CO_2, and at a CO_2 dilution of 57% (MME with CO_2) the CO_2 storage is 5 times greater than it would be with CH_4 dilution. The increased storage is due to an increase in the density of the injected gas in addition to the obvious effect of the increase in CO_2 concentration.

Reservoir Flow Mechanics

The fraction of the pore space that can be filled with injection gas is controlled largely by reservoir heterogeneity, gravity segregation, and the efficiency that injected gas displaces whatever pore fluids are present. High pressure CO_2, whether or not it is diluted with other components, will have a viscosity of a few hundredths of a centipoise at best. Fluid mobility in porous media is inversely proportional to viscosity. Hence, the highly mobile injection gas will find any preferential flow paths that exist in the reservoir. Vertical flow induced by the difference in density between the injected gas and the oil and water present in the reservoir can modify the effects of heterogeneity, though it rarely eliminates them.

A series of reservoir simulations illustrates the interactions between reservoir heterogeneity, mobility of injected and resident fluids, gravity, and phase behavior. First, simulation will be used to illustrate the effect of reservoir heterogeneity on flow paths within a reservoir. Then increasing degrees of realism and complexity will be added to the simulation. Successive cases show the coupling of heterogeneity with the adverse mobility ratio characteristic of gas injection into oil reservoirs, the effect of gravity, and finally all of the previous factors combined with full interaction of multiphase flow with phase behavior.

For this portion of the study we use Eclipse, a commercially available reservoir simulator. For initial work we use Eclipse 100 and for fully compositional simulations, Eclipse 300. Table 2 details the properties of the oil phase, injection gas, and injection water. Figure 3 shows the two-dimensional permeability field for simulations (2001 SPE Comparative Solution Project). The permeability field is characteristic of a sandstone reservoir with strong correlation of permeability in the horizontal direction. Shading indicates the magnitude of permeability according to the scale shown. For the calculations reported below, the permeability field is represented by 20 grid blocks in the vertical direction and 100 grid blocks in the horizontal direction. The dimensions of the field is 762m*15.24m*7.62m (L*H*D) with a porosity of 0.2. Figure 4 details the relative permeability for water, oil, and gas. In order to focus on the flow effects we assume that the gas is first contact miscible, and therefore the gas-liquid relative permeabilities are made straight lines with endpoint values of 1. The water-oil relative permeability curves are representative of a strongly water-wet rock.

Heterogeneity, Fluid Mobility, and Gravity Segregation

In the first example, the viscosity of the injection gas and the oil within the simulation volume are set equal as are the densities of each phase. Thus, any nonuniform flow is caused by the heterogeneous permeability field. Gas is injected continuously at a rate of 7 m^3/day (0.3 m/day) across the entire vertical interval of the reservoir. The production well is similarly completed. Saturation maps at successive times in Fig. 5a display the distribution of fluid within the reservoir. Dark red shading indicates oil-filled pore space, whereas dark blue shading indicates injected gas. The displacement is relatively efficient because the ratio of fluid mobilities is unity, and hence, the displacement is stable. Gas breakthrough at the producer is also relatively late. Nevertheless, the injected fluid finds the high-permeability path with least resistance and flows preferentially through it. In field applications of gas injection, it is often the presence of such paths that limits the total amount of gas injected, because continued gas injection can lead to cycling and reinjection of gas with attendant handling and compression costs.

Next, more realistic fluid mobilities are employed. The oil viscosity is roughly 2 cp while the injected gas viscosity is of order 0.05 cp. As illustrated in Fig. 5b, the relatively mobile gas results in an unstable displacement such that gas finds the preferential flow paths within the reservoir. Gas breakthrough at the production well occurs at less than 0.2 PV of gas injected. Again red shading indicates oil-filled pore space and blue, gas-filled pore space. We note that this result depends strongly on the particular heterogeneous reservoir permeability distribution, and hence is quite system dependent. Gas breakthrough time depends critically on the distribution of permeability within a reservoir and the relative permeability of each phase, among other factors. Nevertheless, early gas breakthrough is a common problem for CO_2 EOR. It is likely to require careful consideration in the design of CO_2 storage schemes that cooptimize oil production and CO_2 storage. Figure 5b also demonstrates that the CO_2 content of a reservoir continues to increase after breakthrough, albeit more slowly than prior to breakthrough. CO_2 storage can be increased substantially after breakthrough, but at the cost of significant reinjection of produced gas.

The combined effect of heterogeneity, mobility of fluid phases, and gravity is shown in Fig. 5c. The gas specific gravity is approximately 0.4 at reservoir conditions while the oil gravity is roughly 0.9. The density difference contributes to some gravity segregation of the injected gas as the gas finds the preferential flow path high in the reservoir. Often, however, high to low vertical (upward) transitions in permeability aid the distribution of gas. The low permeability regions serve to disperse the gas within the reservoir if gas can be forced to initially invade the lower part of the reservoir.

These three cases serve to make an important point. Even though the microscopic storage efficiency is quite high because of the straight-line gas-liquid relative permeability functions, the macroscopic reservoir storage efficiency is reduced through the combination of heterogeneity, adverse mobility ratio, and gravity segregation.

Flow Mechanics and Phase Behavior

Phase behavior is a critical factor determining the effectiveness of a reservoir to store CO_2. In the previous simulations, the injected gas was not soluble in the oil. A fully compositional approach is followed next and Eclipse 300 is used. Figure 6 shows the progress of gas injection for the same permeability field and conditions as used in Fig. 5. Again, injection and production wells are completed over the entire reservoir column. The addition of the full compositional details for the oil and gas predicts that the displacement becomes more efficient. The gas breakthrough time is increased and the mass of CO_2 stored increases. This behavior results from the more realistic representation of the phase saturations and relative permeabilities at the displacement pressure, which in this case is just below the MMP. In the current case, the MMP of the oil-gas system is equivalent to the compositional system used for the gas enrichment studies.

For reference, a waterflood was also simulated for this case. The volumetric water injection rate was made the same as the gas injection rate. Water actually does a fairly good job of displacing oil because the water and oil viscosities are nearly identical. There is, however, no storage of CO_2 with the waterflood. Figure 7 summarizes the cumulative oil-recovery behavior for all of the scenarios discussed thus far. Generally, recovery resulting from the black oil simulations of continuous gas injection decreases as the physical processes simulated become more complicated and realistic. However, the compositional effects included in the E300 simulation act in favor of the oil recovery due to the interactions between the oil in place and the injection gas.

Finite Difference versus Streamline Simulation

The previous examples demonstrate that simulating CO_2 flow behavior in reservoirs is difficult because of the interplay between miscibility, composition, and reservoir heterogeneity, and the computational demands these aspects impose. Nevertheless, simulation will play a vital role as a means to design storage schemes and for evaluating uncertainty. For example, a reservoir permeability field is never known with any certainty and the flow behavior of several different realizations of geology must be computed to gauge the range of possible behavior.

Fully-compositional, finite-difference simulation techniques are intractably slow for full scale reservoir simulation, especially when the number of chemical components is made relatively large and grid dimensions are made sufficiently fine to begin to resolve the coupling between flow and phase behavior (Batycky *et al.* 1997). Streamline methods hold great promise for aiding the design of efficient injection and storage processes, as well as deciding the best time to halt production from an aging reservoir while allowing it to continue to fill with CO_2. (c.f., Higgins and Leighton, 1962; Batycky *et al.*, 1997; Hewett and Yamada, 1997). Streamline methods are based on the idea that the flow can be represented by a series of 1D displacements along streamlines or streamtubes. Thus, the dimensionality of the problem is reduced greatly. A streamline is tangent everywhere to the instantaneous velocity field and perpendicular to isopotential lines. The effects of heterogeneity and evolving flow paths are captured by the locations of streamlines. The physical and chemical mechanisms of the displacement are captured in detail by the 1D flow model.

Figure 8 shows the results of a gas displacement calculated with a streamline simulator for the same permeability field and compositional fluid description as in Fig. 6. For this comparison the permeability field is taken to be horizontal in order to demonstrate the areal displacement efficiency and to eliminate the effects of gravity segregation. Gas is injected from a horizontal well completed over the entire width of the geometry, whereas oil/gas is produced from another horizontal well also completed over the entire width of the geometry.

The streamline simulator calculates one-dimensional (1D) solutions for flow along each streamline and updates streamlines periodically to account for changes in fluid mobility. Streamline simulators have been shown to be much faster than conventional finite difference methods for flows (such as those dominated by heterogeneity) in which streamlines do not change rapidly (Thiele *et al*. 1996). In addition, the streamline simulations are affected much less by numerical dispersion, which alters composition paths in a nonphysical way, than are conventional finite difference calculations. The version of the simulator described by Thiele *et al*. was modified to replace a numerical solution of the 1D flow problem with the semi-analytical approach developed by Jessen *et al*. (1999). Use of the fast 1D solver of Jessen *et al*. permits calculations with enough components that the phase equilibrium for a gas/oil system can be represented with reasonable accuracy. For comparison, the results from mapping 1D finite-difference solutions along streamlines with use of 25 and 100 grid blocks to obtain the 1D solutions are shown along with conventional, compositional, finite-difference simulation results. The finite difference simulator requires 61 min to run the problem whereas the streamline simulator with analytical solution of the 1D flow problem completes the simulation in less than 1min. For 3D problems, the speed-ups will be much larger than they are for this relatively small computational problem. Figure 9 shows the fraction of the pore space occupied by injected gas as well as the fraction occupied by CO_2. As in previous cross-sections, red denotes oil and blue denotes gas-filled pore space. In all cases after breakthrough of the injected gas, the volume of pore space occupied by CO_2 continues to rise as the lower permeability portions of the reservoir are swept more slowly. There is substantial numerical dispersion in the saturation field of the conventional finite difference simulation. Numerical dispersion arises from truncation error in the finite difference representation. In compositional simulations of near-miscible systems, it causes the composition path to move away from the critical locus, and hence it alters displacement efficiency by changing saturations. Comparison of the streamline and E300 simulations indicates that considerable numerical dispersion must be added to make the streamline results match the E300 results. Thus, not only is the streamline methods much more efficient computationally, it is also more accurate. Research is underway now to develop a 3D version of the compositional code that includes the effects of gravity. In the following section, reservoir engineering schemes will be discussed for increasing CO_2 storage.

Increasing CO_2 Storage

A technique that may aid storage capacity is the partial completion of both injection and production wells as well as the use of horizontal wells to distribute gas and produce oil. Here we illustrate only partial completions. In the presence of buoyancy and mobility effects completing injection wells low in the formation rather than over the entire reservoir column improves the contact of gas with the reservoir volume. Gas that is injected low in the formation will disperse while rising as it encounters high to low permeability transitions. A production well that is completed low in the formation will also delay gas breakthrough time and reduce the producing gas-oil ratio because the gas and oil will tend to remain segregated by gravity in the formation. Likewise, ensuring that a production well is not completed opposite to a high-permeability region of the formation will reduce the tendency of injected gas to channel between injector and producer. Figure 10 reports the effect on oil recovery and CO_2 storage for two completion strategies. In the first case, the injection and production wells are completed over the entire reservoir column. In the second case, the injection well is partially completed while the production well is open over the entire reservoir column. Dashed lines represent the storage factor while solid lines are cumulative oil recovery. The partial completion scheme increases both the CO_2 storage capacity and the cumulative oil production by a modest amount. A second example of the effect of completions is shown in Figure 11, this time calculated by compositional simulations. Replacing the full vertical completion of the injector with completions in the top and bottom three grid blocks also increase oil recovery and CO_2 storage. These examples indicate again that the key limiting factor for both oil production and CO_2 storage is the cycling of gas due to heterogeneity.

Conventional gas injection processes often include water injection as well. Such schemes are generally called WAG (water alternating gas) injection, and there are a number of variations commonly used. In one version alternate slugs of water and gas are injected. In another, gas is injected continuously until significant breakthrough occurs. At that point WAG injection begins. The benefits of WAG injection arise from two sources. First, and usually most important, gravity forces cause the water and gas to sweep different portions of the pore space. Generally gas invades upper portions of the reservoir more effectively while water invades the lower portion more effectively. In addition, presence of water in preferential flow paths can reduce the mobility of the gas, hereby reducing gas cycling.

Figure 12 and 13 demonstrate the ability of WAG to increase CO_2 capacity of a reservoir. The figures show results from black-oil simulation of two cases with equal-sized slugs of water and CO_2. In the first case water and gas is injected alternating in slugs of 0.1 PV, whereas the second case uses 0.3 PV slugs. WAG injection gives better oil recovery than the waterflood and offers a reasonable emplacement of CO_2 into the formation. Thus, an obvious parameter to optimize is the WAG ratio, that is, the volumetric flow rate ratio of water to gas in the injected fluid. This optimization is thoroughly reservoir specific because the performance of any WAG scheme depends strongly on the distribution of permeability as well as factors that determine the impact of gravity segregation (fluid densities, viscosities and reservoir flow rates). In addition, the performance of a WAG scheme can depend strongly on the details of the flow behavior of the oil, gas and water as reflected by the two- and three-phase relative permeability. Variables that can be considered include the timing of the switch from gas to water injection, the sizes of the water and gas slugs as well as the injection rates. Further, of course, sequencing of gas, water and WAG injection across a large field can offer significant opportunities for increased gas storage.

Aquifers underlie many oil fields, a fact that suggests a less conventional scheme for CO_2 storage. CO_2 could be injected into the aquifer instead of into the oil zone above. Injection deep in the aquifer would be less prone to cycling, and could displace oil trapped in the vertical capillary transition zone from between water-filled and oil-filled pore space in the upper part of the aquifer. Here again, the specific reservoir situation will determine whether aquifer injection makes sense, but it should be investigated because aquifer volumes can be large. Finally, there will be some point in the economic life of an oil field at which the cost of operating the production wells is unattractively high given the oil production. It would be possible, however, to continue CO_2 injection after the oil production ceases. Most oil fields experience a significant decline in pressure during their producing live. Repressurizing the reservoir would allow substantial additional increase in storage, though the value of oil recovered would no longer offset the cost of CO_2 injection. Slow gravity drainage of remaining oil might also allow periodic production of some additional oil in specific reservoir situations.

Conclusions

Oil fields are likely to be one of the first geologic formations where carbon dioxide (CO_2) is injected for sequestration because the oil industry has considerable experience in the use of CO_2 for oil recovery. Successful CO_2 oil recovery processes, to date, have minimized the mass (or volume) of CO_2 needed to recover a barrel of oil. The problem of increasing CO_2 storage while recovering maximum oil is a complicated, reservoir-specific problem.

The calculations reported here for a specific heterogeneous reservoir suggest the following approaches to increase CO_2 storage:

1 Adjust injection gas composition to maximize CO_2 concentration while maintaining an appropriate MMP.

2 Design well completions (or consider horizontal wells) to create injection profiles that reduce the adverse effects of preferential flow of injected gas through high permeability zones.

3 Optimize water injection (timing, injection rates and WAG ratio) to minimize gas cycling and maximize gas storage.

4 Consider aquifer injection to store CO_2 that would flow rapidly to producing wells if reinjected in the oil zone.

5 Consider reservoir repressurization after the end of the producing life of the field.

References

Batycky, R. P., Blunt, M. J., and Thiele, M.R., “A 3D Field-Scale Streamline-Based Reservoir Simulator,” Soc. Pet. Eng. Reservoir Engineering, 12(4), 246-254, 1997.

Hewett, T.A., and Yamada, T., "Theory for Semi-Analytical Calculation of Oil Recovery and Effective Relative Permeabilities Using Streamtubes," *Adv Water Resources,* 20(5-6), 279-292, 1997.

Higgins, R. V. and Leighton, A. J., "A Computer Method to Calculate Two-Phase Flow in Any Irregularly Bounded Porous Medium," *J. Pet. Tech.*, June, 679-683, 1962.

Jessen, K. 2000 “Effective Algorithms for the Study of Miscible Gas Injection Processes,” PhD Dissertation, Danish Technical University.

Jessen, K., Ermakov, P., Zhu, J., and Orr, F.M., Jr. 1999 "Fast, Approximate Solutions for 1D Multicomponent Gas Injection Problems," SPE 56608 presented at the 1999 SPE Annual Technical Conference, Houston, Oct. 3-6.

Jessen, K., Michelsen, M.L., and Stenby, E.H. 1998 “Global Approach for Calculation of Minimum Miscibility Pressure,” *Fluid Phase Equilibria* 153, 251-263.

Moritis, G., "1998 Worldwide EOR Survey," *Oil and Gas J.*, Apr. 20, 49-97, 1998.

Orr, F.M., Jr., Dindoruk, B., and Johns, R.T. 1995 “Theory of Multicomponent Gas/Oil Displacements,” *Ind. Eng. Chem. Res.* 34, 2661-2669.

Stevens, S. H. and Gale, J., “Geologic CO_2 Sequestration May Benefit Upstream Industry”, *Oil and Gas J.*, May 15, 40-44, 2000.

2001 SPE Comparative Solution Project. Http://www.pet.hw.ac.uk/3frame.html

Taber, J.J., Martin, F. D., and Seright, R.S., “EOR Screening Criteria Revisited—Part 1: Introduction to Screening Criteria and Enhanced Recovery Field Projects,” *Soc. Pet. Eng. Res. Eng.*, Aug, 189-198, 1997A.

Taber, J.J., Martin, F. D., and Seright, R.S., “EOR Screening Criteria Revisited—Part 2: Applications and Impact of Oil Prices,” *Soc. Pet. Eng. Res. Eng.*, Aug, 199-205, 1997B.

Thiele, M R.,.Batycky, R. P., Blunt, M. J., and Orr, F. M. Jr., “Simulating Flow in Heterogeneous Systems Using Streamtubes and Streamlines,” *Soc. Pet. Eng. Res. Eng.,* Feb, 5-12, 1996.

Wang, Y. and Orr, F.M., Jr. 2001 “Calculation of Minimum Miscibility Pressure,” *J. Pet. Science and Engineering*, 27:151-164, 2000

Zick, A.A. 1986 “A Combined Condensing/Vaporizing Mechanism in the Displacement of Oil by Enriched Gas,” paper SPE 15493 presented at the 1986 SPE Annual Tech. Conf., New Orleans, Oct. 5-8.

Component	Oil	Solvent
CO_2	0.062263	0.2218
CH_4	0.344997	0.2349
C_2	0.052176	0.235
C_3	0.036827	0.2745
C_4	0.025663	0.0338
C_5	0.018695	0
C_6	0.045291	0
C_7	0.164759	0
C_{13}	0.099736	0
C_{19}	0.07414	0
C_{27}	0.046281	0
C_{38}	0.029172	0

Table 1: Oil and solvent compositions used in for the compositional studies. The full fluid description is given in *Jessen et al. (1998)*

P (bar)	Rs	Bo	μ_{oil}	Bg	μ_{gas}
30	33.88	1.1540	3.840230	0.038661	0.016714
50	45.35	1.1805	3.492039	0.022526	0.017716
75	59.50	1.2122	3.109178	0.014547	0.019853
100	73.86	1.2438	2.772320	0.010628	0.023447
125	88.63	1.2761	2.475066	0.008334	0.028630
150	103.95	1.3095	2.212863	0.006852	0.034679
175	119.91	1.3442	1.981486	0.005834	0.040688
200	136.63	1.3823	1.807667	0.005105	0.046274
225	-	1.3801	1.900920	-	-
250	-	1.3771	1.994195	-	-
275	-	1.3722	2.087451	-	-
300	-	1.3675	2.180652	-	-
325	-	1.3631	2.273763	-	-
350	-	1.3589	2.366751	-	-
375	-	1.3549	2.459587	-	-
400	-	1.3511	2.552242	-	-

Table 2: Physical gas-oil properties for black-oil simulations.

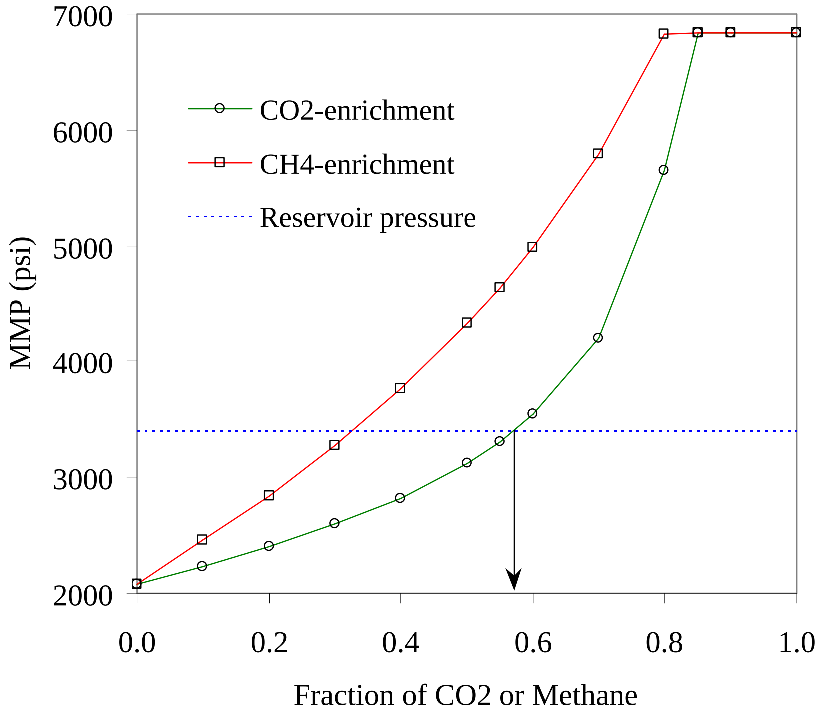

Figure 1: Minimum miscibility pressures for mixtures of solvent (Table 1) and pure CO_2 or pure CH_4.

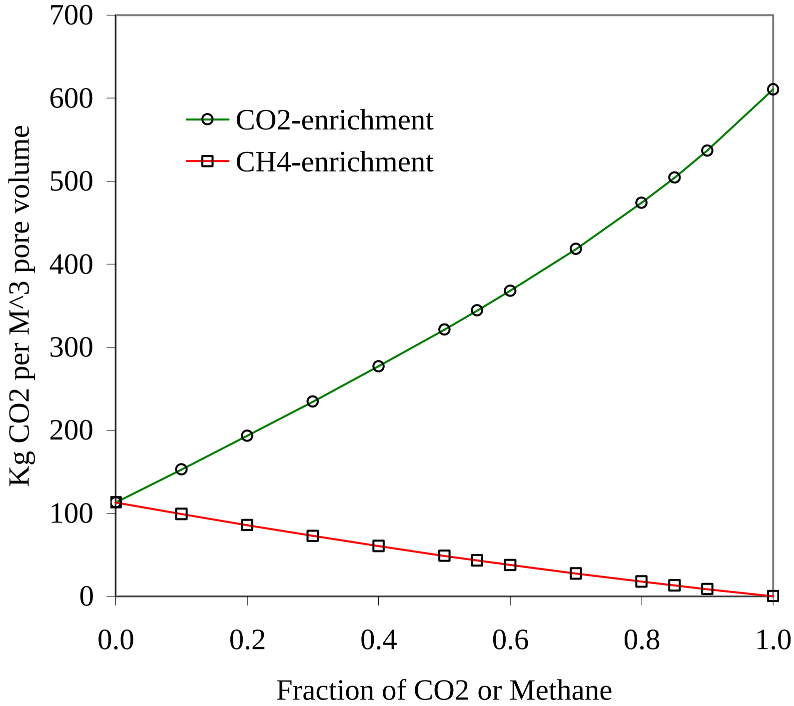

Figure 2: CO_2 storage capacity versus composition of injectant.

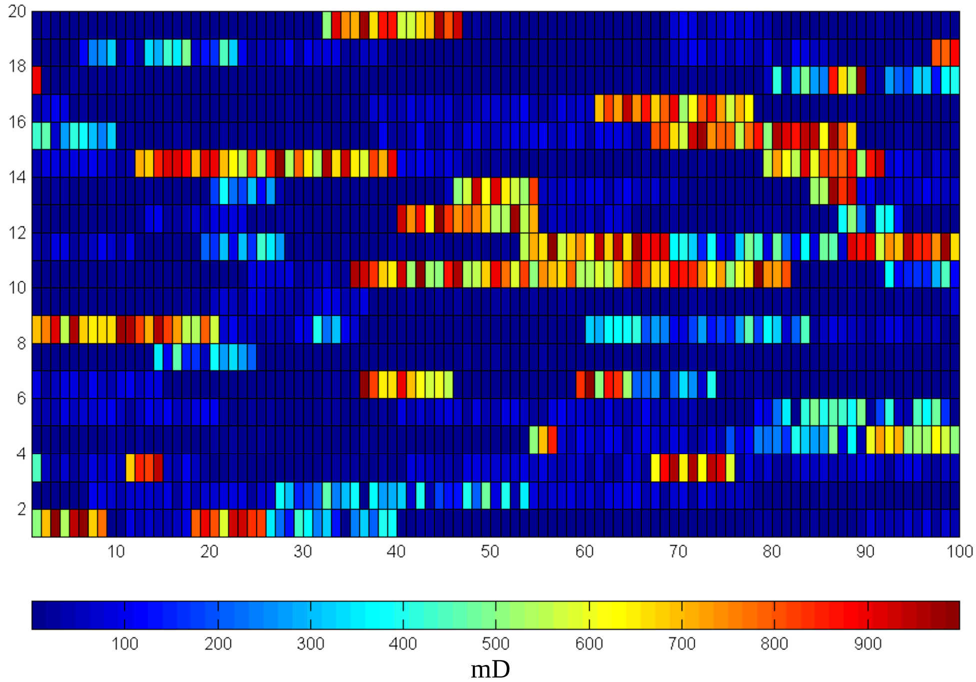

Figure 3: Permeability field used for simulations.

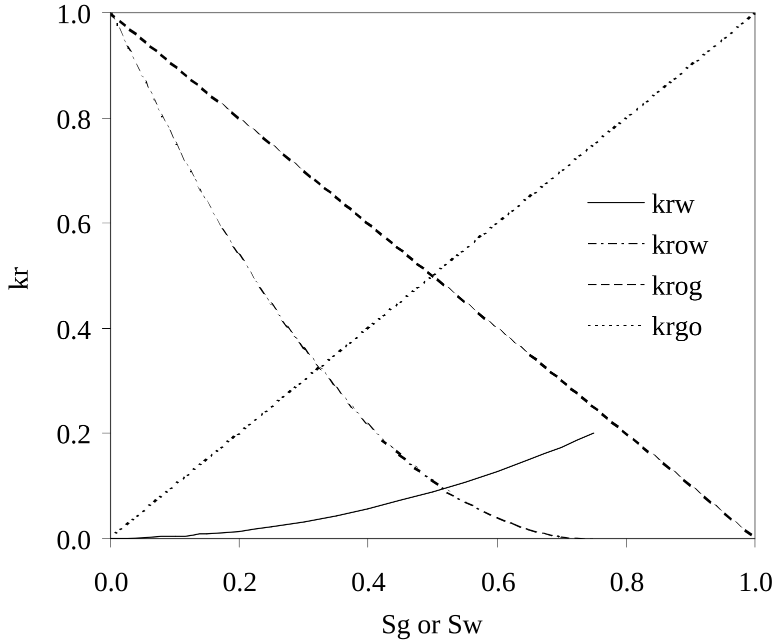

Figure 4. Two-phase relative permeability functions. The Stone 1 approach is used for modeling 3-phase flow of oil, gas and water.

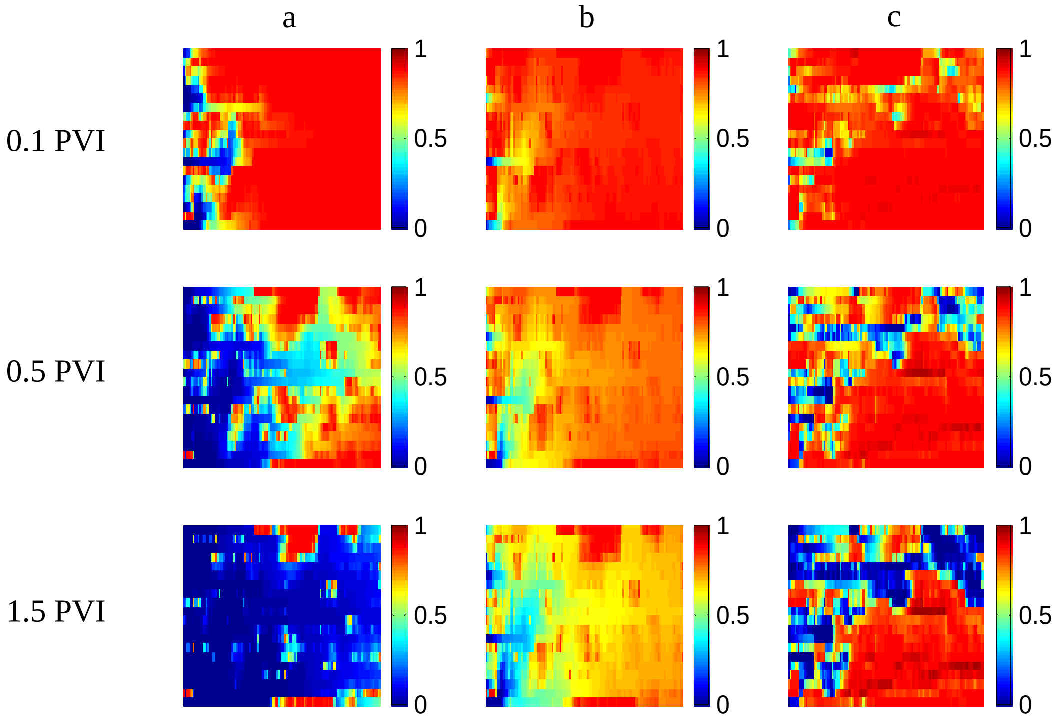

Figure 5: Saturation maps from black-oil simulation of gas injection (a) effect of heterogeneous flow field, (b) effect of heterogeneity and mobility, (c) effects of heterogeneity, mobility and gravity.

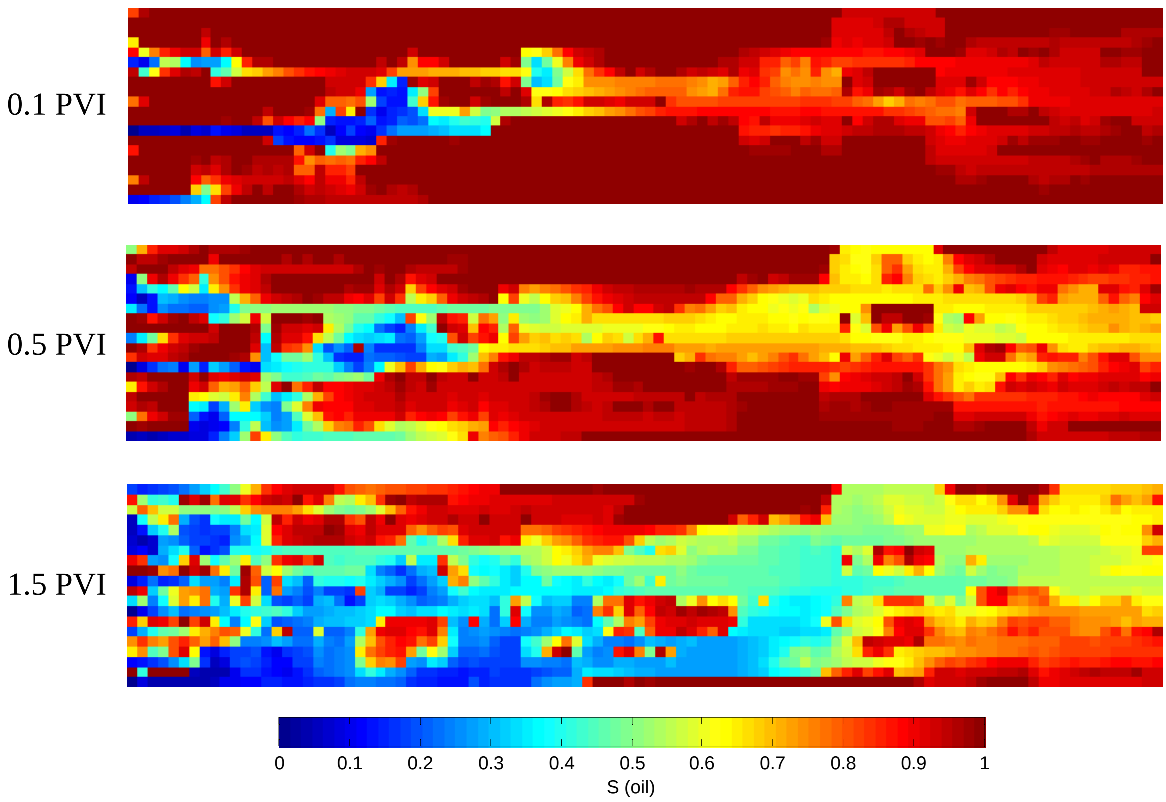

Figure 6: Snapshots from compositional simulation of vertical displacement. Oil saturation.

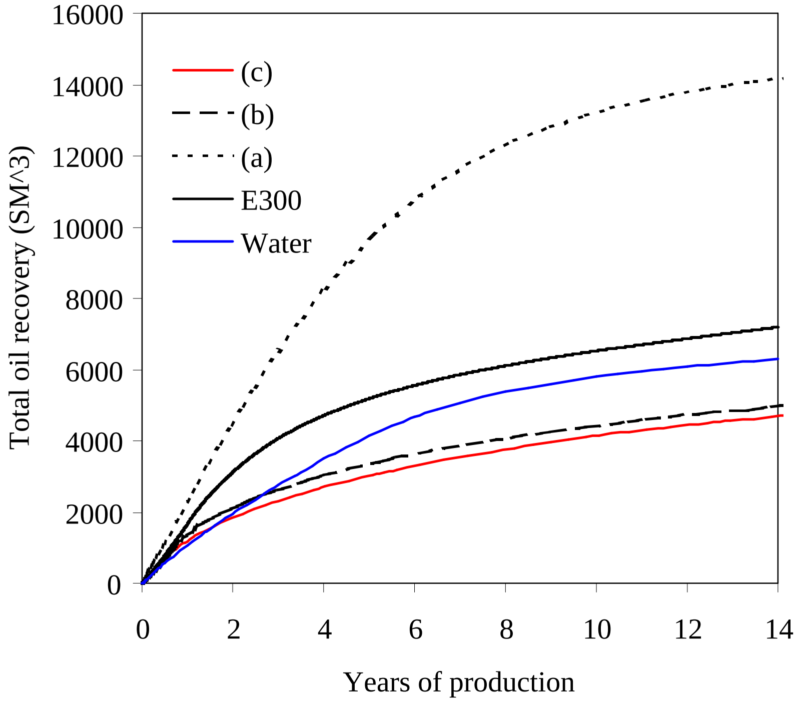

Figure 7: Total oil production for the black-oil cases given in Figure 5 along with waterflood and E300 results.

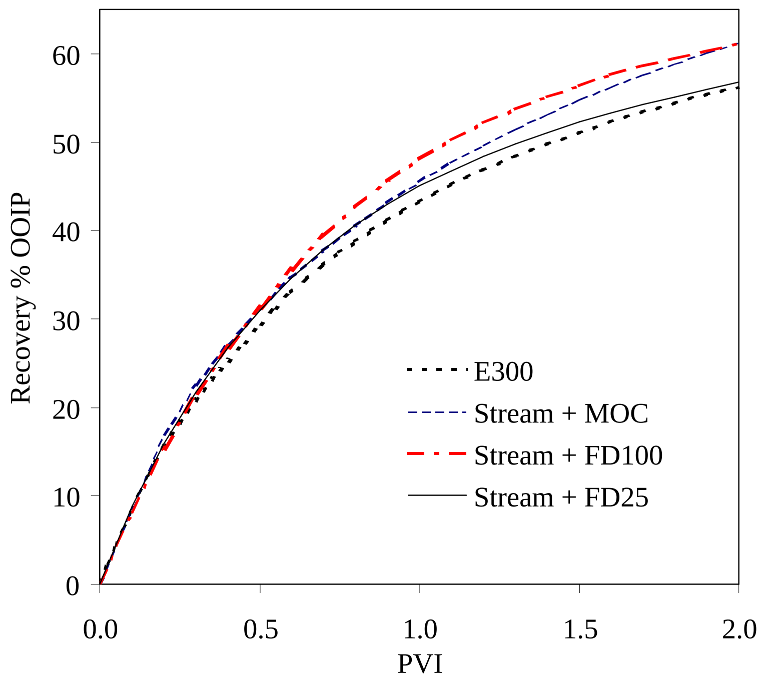

Figure 8: Compositional simulation of areal geometry. Comparison of an Eclipse 300 simulation with Streamtube/1D simulations.

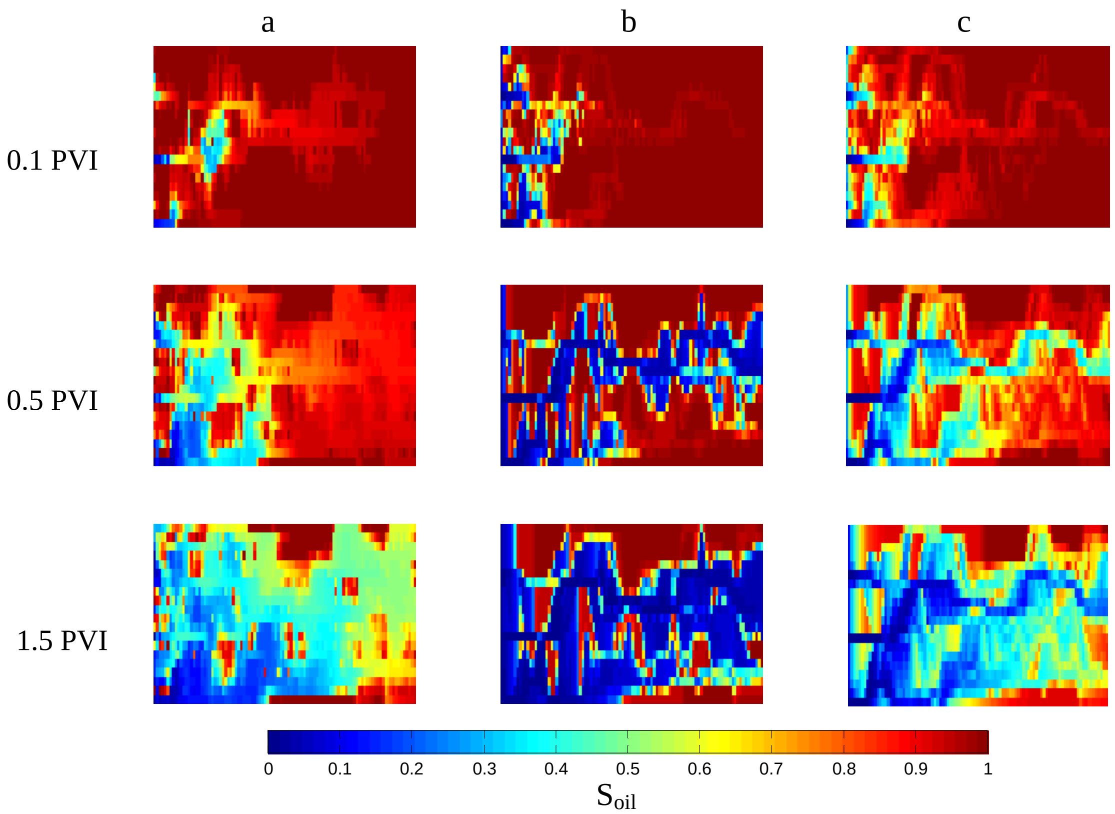

Figure 9: Saturation maps of a) E300 simulation, b) Streamtube simulations using true dispersion-free 1D solutions and c) dispersed 1D solution.

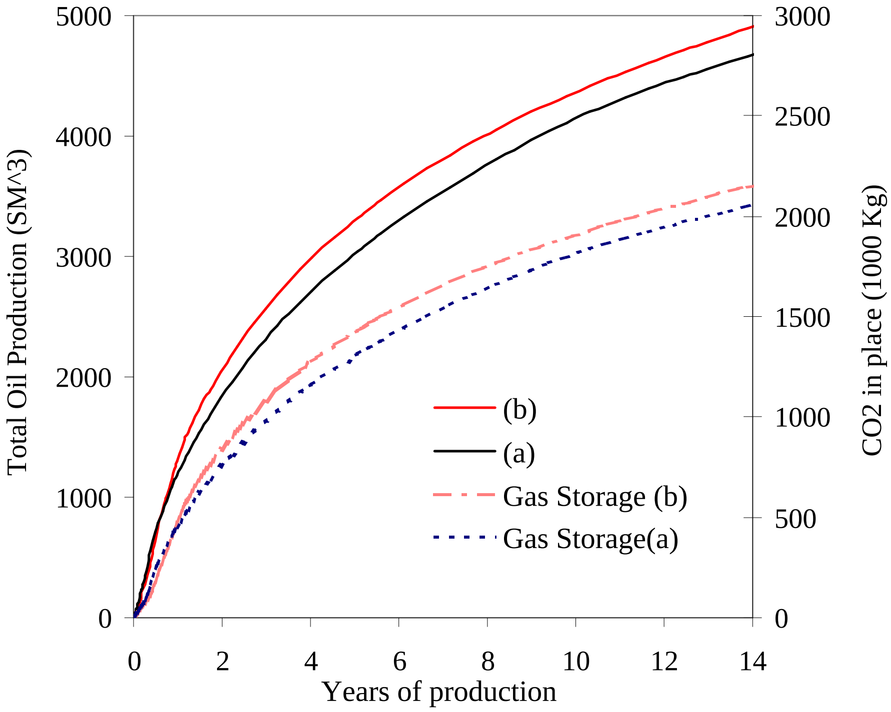

Figure 10: Oil production and CO_2 storage versus time for two black oil cases:

a) Injector completed over the entire reservoir column.

b) Injector completed in the bottom three grid blocks.

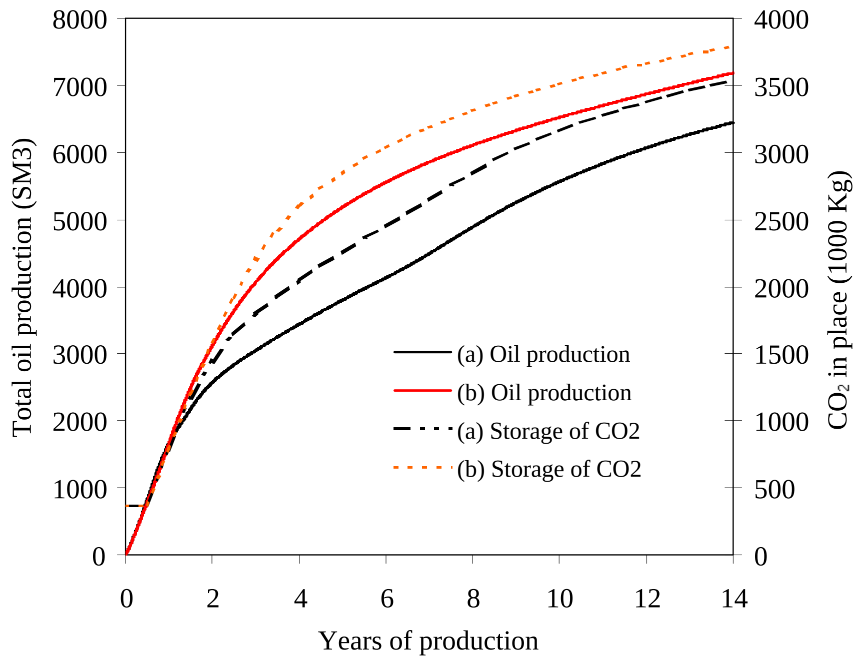

Figure 11: Compositional simulation (E300) of vertical slap geometry:
a) Injector completed over the entire reservoir column.
b) Injector completed in the three top and bottom grid blocks.

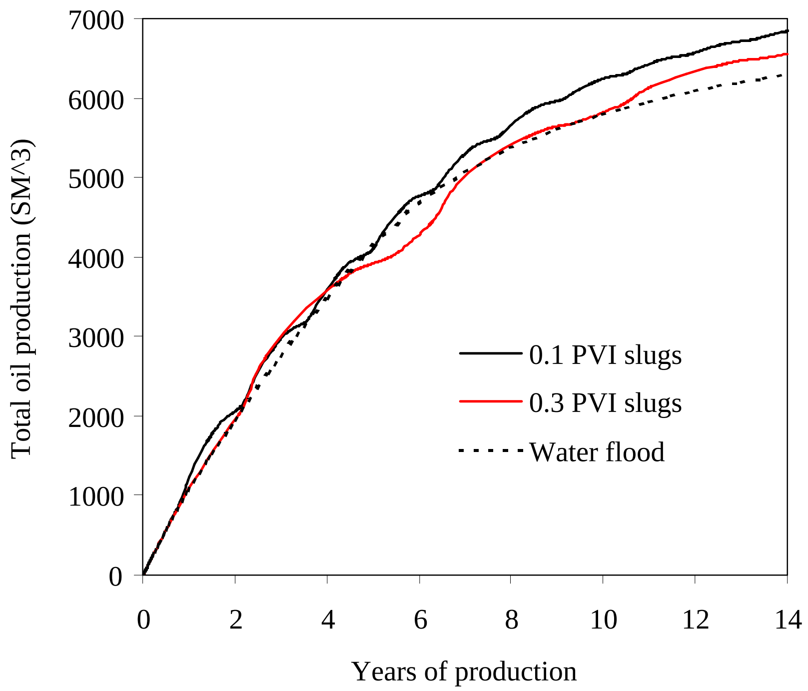

Figure 12: Oil production from waterflood and WAG schemes.

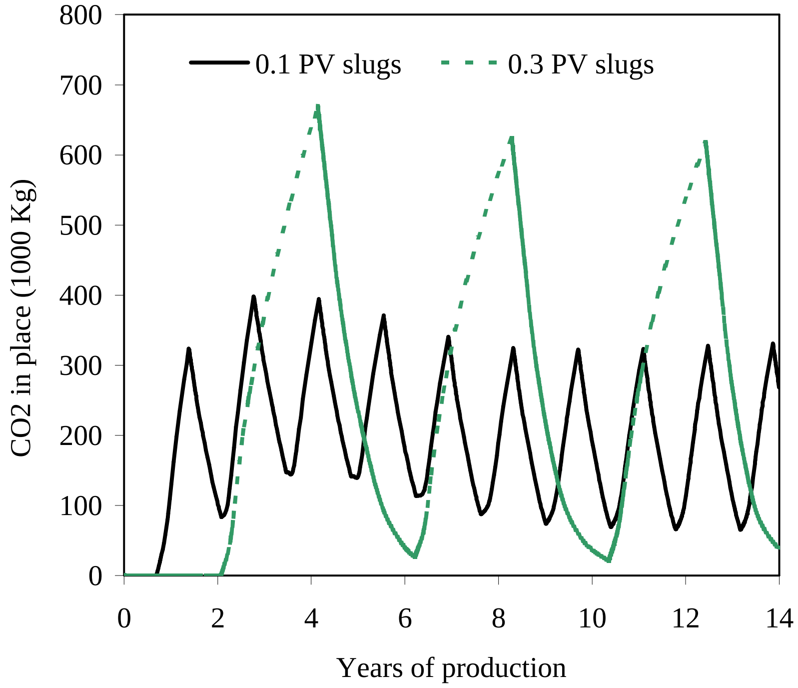

Figure 13: CO_2 storage capacity for WAG schemes.